An Iterative Linear Transformation Algorithm for Solution of the Collinearity Equations

A. J. Naftel and *J. C. Boot*
University of Bradford, Bradford, West Yorkshire BD7 1DP, England

ABSTRACT: A modification of the direct linear transformation (DLT) technique for solving the collinearity equations is proposed. The iterative linear transformation (ILT) procedure involves incorporating photo-coordinate observations of non-control points in the least-squares adjustment leading to the determination of the calibration parameters. The reconstructed object-space coordinates so obtained in a subsequent adjustment are then treated as "approximate" control and the computation is repeated until convergence is obtained. In a study utilizing check-point control, the algorithm reduced the average root-mean-square (RMS) error in the conventional DLT solution from 3.3mm to 0.9mm in 16 iterations. This equates to a spatial resolution of 0.047 percent (about 1 part in 2130) in object-space dimensions. Applications to two test surfaces requiring reconstruction of a much larger number of spatial points yielded similar reductions in average RMS errors in 50 and 140 iterations, respectively.

INTRODUCTION

IN RECENT YEARS the direct linear transformation (Abdel-Aziz and Karara, 1971), 11-parameter (Bopp and Krauss, 1978), self-calibration (Fraser, 1982), and bundle adjustment (Granshaw, 1980) methods have all been proposed as competing techniques for solution of the collinearity equations in close-range photogrammetry.

Fraser (1982) has demonstrated that relative accuracies of 1:10,000 and higher in the object space an be achieved with the self-calibration / bundle adjustment technique as opposed to 1:6,000 for a direct linear transformation (DLT) type procedure.

Apart from its potential for greater accuracy, the bundle adjustment method holds a number of advantages over competing DLT type solutions:

- Flexibility resulting from an ability to combine photogrammetric and surveying observations simultaneously in the adjustment.
- Lack of necessity to provide highly redundant object-space control.
- Modeling of systematic errors such as lens and film distortion without recourse to making specific additional observations for this purpose.
- Strong agreement between estimates of precision as given by statistical indicators such as root-mean-square (RMS) errors and accuracy determined with respect to check-point control.

The main disadvantages relate to the computational expense required to achieve a solution in terms of time and storage, and the need for initial approximations to unknown parameters.

Conversely, the DLT approach offers the following attractions:

- Substantially less computer resources are required.
- Being a direct method, no initial approximations are needed.

The disadvantages of the DLT method are that it depends on the provision of a large redundant control-point configuration (particularly if high accuracy is demanded), and it does not lend itself to rigorous statistical analysis because standard errors quoted are often over optimistic (Fraser, 1982). The latter observation arises because the DLT equations contain 11 independent parameters compared to nine in the original collinearity condition. In general, this approximation violates orthogonality of the transformation between object space and image coordinate systems implicit in the collinearity restraint, thus resulting in spatial reconstruction errors. This anomaly was later rectified by Bopp and Krauss (1978) who placed the method on a more rigorous mathematical footing by introducing two nonlinear constraints between the 11 DLT parameters. More recently, Hatze (1988) has shown that incorporation of at least one of the constraints in linearized form leads to a significant reduction in reconstruction errors.

It has been pointed out, however, that, in the presence of a "healthy degree" of redundant control, the DLT and 11-parameter solutions can be assumed equivalent for practical purposes (Granshaw, 1980). Therefore, in applications where the provision of a significant number of accurately coordinated control points presents no appreciable problems, adoption of the DLT technique need not lead to any significant loss in accuracy. For this reason the DLT method has proved particularly appealing in biomechanical applications of close-range photogrammetry (Shapiro, 1978; Van Gheluwe, 1978; Alem *et al.*, 1978; Miller *et al.*, 1980).

In this paper, therefore, we first review the DLT approach and the limitations in the original computer implementation of it (Marzan and Karara, 1975). We then present a modified algorithm which addresses these criticisms and improves the accuracy of the reconstruction, while still preserving the overall advantages of the technique. Finally, performance of the new algorithm is demonstrated with reference to a number of experimental studies.

OUTLINE OF THE DIRECT LINEAR TRANSFORMATION (DLT) PROCEDURE

The collinearity condition may be expressed by the following equations (Marzan and Karara, 1975):

$$
\begin{aligned}
x + \Delta x - x_0 &= -C_x \frac{\{m_{11}(X-X_0) + m_{12}(Y-Y_0) + m_{13}(Z-Z_0)\}}{\{m_{31}(X-X_0) + m_{32}(Y-Y_0) + m_{33}(Z-Z_0)\}} \\
y + \Delta x - y_0 &= -C_y \frac{\{m_{21}(X-X_0) + m_{22}(Y-Y_0) + m_{23}(Z-Z_0)\}}{\{m_{31}(X-X_0) + m_{32}(Y-Y_0) + m_{33}(Z-Z_0)\}}
\end{aligned} \tag{1}
$$

with $C_x = C/\lambda_x$; $C_y = C/\lambda_y$

where X,Y,Z are the three-dimensional spatial coordinates of a point in space;
x,y are the observed comparator coordinates of the image of the point in the photograph;
x_0,y_0 are the photo coordinates of the principal point;
X_0,Y_0,Z_0 are the spatial coordinates of the camera perspective center;
m_{ij} are the elements of the 3 by 3 orthogonal rotation matrix;
C denotes the principal camera distance;
λ_x,λ_y are scale factors for the x,y comparator coordinate axes; and

PHOTOGRAMMETRIC ENGINEERING & REMOTE SENSING,
Vol. 57, No. 7, July 1991, pp. 913-919.

0099-1112/91/5707–913$03.00/0

$\Delta x, \Delta y$ are the systematic errors in the comparator coordinates.

The systematic error terms Δx, Δy can be ascribed to the nonlinear components of symmetrical and asymmetrical lens distortion, and take the following form:

$$\begin{aligned} \Delta x &= x'(K_1r^2+K_2r^4+K_3r^6+\ldots)+P_1(r^2+2x'^2)+2P_2x'y' \\ \Delta y &= y'(K_1r^2+K_2r^4+K_3r^6+\ldots)+P_2(r^2+2y'^2)+2P_1x'y' \end{aligned} \tag{2}$$

where $x' = x - x_0$; $y' = y - y_0$; $r^2 = x'^2+y'^2$;
K_1, K_2, K_3 are coefficients of symmetrical lens distortion; and
P_1, P_2 are coefficients of asymmetrical lens distortion.

Abdel-Aziz and Karara (1971) rearranged the parameters in Equations 1 to yield the following relationships:

$$\begin{aligned} x + \Delta x &= \frac{L_1X + L_2Y + L_3Z + L_4}{L_9X + L_{10}Y + L_{11}Z + 1} \\ y + \Delta y &= \frac{L_5X + L_6Y + L_7Z + L_8}{L_9X + L_{10}Y + L_{11}Z + 1} \end{aligned} \tag{3}$$

where L_j, $j=1, \ldots, 11$ are the 11 DLT coefficients.

Equations 3 are known as the DLT equations.

Neglecting the systematic errors in image coordinates, Equations 3 can be written as

$$\begin{aligned} L_1X_i+L_2Y_i+L_3Z_i+L_4-x_i'X_i\,L_9-x_i'Y_i\,L_{10}-x_i'Z_iL_{11}-x_i' &= 0 \\ L_5X_i+L_6Y_i+L_7Z_i+L_8-y_i'X_i\,L_9-y_i'Y_i\,L_{10}-y_i'Z_iL_{11}-y_i' &= 0 \end{aligned} \tag{4}$$

relating the image coordinates (x_i' y_i') of point i to its originial object-space coordinates (X_i, Y_i, Z_i) through the DLT coefficients. Thus, each known object-space (control) point yields two equations in the form of Equations 4. Provided at least six such points are observed in any photograph, its calibration can therefore be undertaken indirectly through the DLT coefficients; redundant control may be used to yield an overdetermined system. Assuming that n control points ($i = 1, \cdots, n$) are employed, the resulting set of equations can be expressed in full matrix form as

$$\begin{bmatrix} X_1 & Y_1 & Z_1 & 1 & 0 & 0 & 0 & 0 & -x_1'X_1 & -x_1'Y_1 & -x_1'Z_1 \\ 0 & 0 & 0 & 0 & X_1 & Y_1 & Z_1 & 1 & -y_1'X_1 & -y_1'Y_1 & -y_1'Z_1 \\ \cdot & \cdot & \cdot & \cdot & \cdot & \cdot & \cdot & \cdot & \cdot & \cdot & \cdot \\ \cdot & \cdot & \cdot & \cdot & \cdot & \cdot & \cdot & \cdot & \cdot & \cdot & \cdot \\ \cdot & \cdot & \cdot & \cdot & \cdot & \cdot & \cdot & \cdot & \cdot & \cdot & \cdot \\ X_i & Y_i & Z_i & 1 & 0 & 0 & 0 & 0 & -x_i'X_i & -x_i'Y_i & -x_i'Z_i \\ 0 & 0 & 0 & 0 & X_i & Y_i & Z_i & 1 & -y_i'X_i & -y_i'Y_i & -y_i'Z_i \\ \cdot & \cdot & \cdot & \cdot & \cdot & \cdot & \cdot & \cdot & \cdot & \cdot & \cdot \\ \cdot & \cdot & \cdot & \cdot & \cdot & \cdot & \cdot & \cdot & \cdot & \cdot & \cdot \\ \cdot & \cdot & \cdot & \cdot & \cdot & \cdot & \cdot & \cdot & \cdot & \cdot & \cdot \\ X_n & Y_n & Z_n & 1 & 0 & 0 & 0 & 0 & -x_n'X_n & -x_n'Y_n & -x_n'Z_n \\ 0 & 0 & 0 & 0 & X_n & Y_n & Z_n & 1 & -y_n'X_n & -y_n'Y_n & -y_n'Z_n \end{bmatrix} \begin{bmatrix} L_1 \\ L_2 \\ \cdot \\ \cdot \\ \cdot \\ \cdot \\ \cdot \\ \cdot \\ \cdot \\ \cdot \\ L_{10} \\ L_{11} \end{bmatrix} = \begin{bmatrix} x_1' \\ y_1' \\ \cdot \\ \cdot \\ \cdot \\ x_i' \\ y_i' \\ \cdot \\ \cdot \\ \cdot \\ x_n' \\ y_n' \end{bmatrix} \tag{5}$$

This system has 2n-11 degrees of freedom, and conforms to the general form

$$\mathbf{K} \cdot \mathbf{X} - \mathbf{r} = \mathbf{v} \tag{6}$$

where **K** is a real $p \times q$ matrix ($p \geqslant q$) of constants of rank q,
r is a column vector of q constants,
X is the column vector of q unknowns, and
v is the vector of q residuals, which for the exact solution to **X** are all zero.

A solution to Equation 6 may be obtained using the principle of least squares as

$$\mathbf{X} = [\mathbf{K}^T \cdot \mathbf{W} \cdot \mathbf{K}]^{-1} \cdot \mathbf{K}^T \cdot \mathbf{W} \cdot \mathbf{r} \tag{7}$$

where **W** is a $p \times p$ weight matrix, the precise form of which for the present application may be found in Marzan and Karara (1975).

The statistical errors in the above solution are usually assessed in terms of the variance-covariance matrix (Wong, 1975) given by

$$\boldsymbol{\sigma}_X 2 = \sigma_0^2\, [\mathbf{K}^T \cdot \mathbf{W} \cdot \mathbf{K}]^{-1} \tag{8}$$

where σ_0^2, the variance of unit weight, is expressed as

$$\sigma_0^2 = \frac{\mathbf{v}^T \cdot \mathbf{W} \cdot \mathbf{v}}{p - q}$$

Thus, a solution for L_j can be obtained using Equations 7 and 8 utilizing any standard mathematical subroutine library.

Following evaluation of the DLT coefficients L_j^k for each of the m obtained images (i.e., $k=1, \ldots, m$), the object space coordinates of the required unknown points can be determined as a multiray intersection problem.

Regrouping the terms in Equations 4 in order to separate the unknown space coordinates (X, Y, Z) of a non-control point, it follows that

$$\begin{aligned} (L_1-x'L_9)X+(L_2-x'L_{10})Y+(L_3-x'L_{11})Z+(L_4-x') &= 0 \\ (L_5-y'L_9)X+(L_6-y'L_{10})Y+(L_7-y'L_{11})Z+(L_8-y') &= 0 \end{aligned} \tag{9}$$

Let (X, Y, Z) represent the cartesian components of an unknown object point with image coordinates (x_k', y_k') and DLT coefficients ($L_1^k, L_2^k, \ldots, L_{11}^k$) referred to a particular photograph k. Assuming that the point is imaged in m photographs ($k = 1, \ldots, m$), Equations 9 can be re-written in the form

$$\begin{bmatrix} (L_1^1-x_1'L_9^1) & (L_2^1-x_1'L_{10}^1) & (L_3^1-x_1'L_{11}^1) \\ (L_5^1-y_1'L_9^1) & (L_6^1-y_1'L_{10}^1) & (L_7^1-y_1'L_{11}^1) \\ \cdot & \cdot & \cdot \\ \cdot & \cdot & \cdot \\ \cdot & \cdot & \cdot \\ (L_1^k-x_k'L_9^k) & (L_2^k-x_k'L_{10}^k) & (L_3^k-x_k'L_{11}^k) \\ (L_5^k-y_k'L_9^k) & (L_6^k-y_k'L_{10}^k) & (L_7^k-y_k'L_{11}^k) \\ \cdot & \cdot & \cdot \\ \cdot & \cdot & \cdot \\ \cdot & \cdot & \cdot \\ (L_1^m-x_m'L_9^m) & (L_2^m-x_m'L_{10}^m) & (L_3^m-x_m'L_{11}^m) \\ (L_5^m-y_m'L_9^m) & (L_6^m-y_m'L_{10}^m) & (L_7^m-y_m'L_{11}^m) \end{bmatrix} \begin{bmatrix} X \\ Y \\ Z \end{bmatrix} = \begin{bmatrix} -(L_4^1-x_1') \\ -(L_8^1-y_1') \\ \cdot \\ \cdot \\ \cdot \\ -(L_4^k-x_k') \\ -(L_8^k-y_k') \\ \cdot \\ \cdot \\ \cdot \\ -(L_4^m-x_m') \\ -(L_8^m-y_m') \end{bmatrix} \tag{10}$$

Equations 10 have $2m-3$ degrees of freedom, and can therefore be solved to yield X, Y, Z coordinates for each point on the object surface, using a second least-squares adjustment. Again, the appropriate form of the weight matrix is given by Marzan and Karara (1975).

The computer implementation of the above procedure, as presented by Marzan and Karara (1975), obtains an initial solution to Equations 5 using Equations 7 by awarding unit weight to all equations. The resulting set of DLT parameters is then used to yield an updated weight matrix taking account of the consistency with which each equation fits the overall solution according to Equation 8; Equation 7 is then used to obtain a second solution to Equations 5. A solution for the required unknown object space points is then obtained from Equations 10 using Equation 7 in essentially the same manner.

This program, which has apparently been used extensively since (Miller *et al.*, 1980; Wood and Marshall, 1986) without modification, suffers from the following limitations:

- Photocoordinate observations of non-control points are not directly incorporated in the least-squares adjustment leading to the determination of the DLT and (when utilized) additional distortion parameters (ADPs). Thus, a useful source of redundant information is wasted.
- It is a direct approximate method. Thus, there is no facility for successive improvement of the obtained solution, which is therefore a strong function of the object space and control configuration.

Modifications to the DLT procedure are now suggested, with the aim of alleviating the above restrictions.

FORMULATION OF THE ILT (ITERATIVE LINEAR TRANSFORMATION) METHOD

In order to improve the performance of the existing DLT program, the following modifications are proposed:

(1) An initial solution to the unknown object-space coordinates through Equations 5, 7, and 10, assuming unit weight matrices, can be readily obtained using one of the standard mathematical subroutine libraries that are currently available.

(2) The initial solution for the unknown object-space coordinates is then fed directly back into Marzan and Karara's program, along with the known control-point coordinates which are maintained constant. Thus, photocoordinate observations to non-control points are used in an adjustment leading to the solution of the calibration parameters, which has a greater degree of redundancy. Although this makes full use of the newly available redundant equations involving the non-control points and DLT parameters, it must be appreciated that the control and non-control points have, in all probability, been surveyed to different degress of accuracy. Nevertheless, reformulating the weight matrix as previously described automatically ensures that each equation is awarded a weighting according to its consistency with the previously obtained overall solution. As a consequence, a more robust solution to the object-space coordinates of the unknown reconstructed points can now be computed.

(3) It would then appear natural to allow the compound DLT solution to the object-space coordinates to serve as a better trial approximation to the coordinates of the unknown points and allow the procedure to be repeated in an iterative fashion. In the process, a direct solution technique has been converted into a simple iterative scheme and the DLT can be re-christened appropriately as the ILT (iterative linear transformation) method.

The proposed modifications to the DLT scheme can be expressed more formally. When the image coordinates of all n control points (i.e., $j = 1,\ldots, n$) recorded on a given photograph are substituted in turn into Equations 5, the resulting set of $2n$ equations can be expressed in matrix form as

$$[A_n(\mathbf{x}_j',\mathbf{X}_j)]\ \mathbf{L}^0 = \mathbf{b}_n(\mathbf{x}_j') \tag{11}$$

where $\mathbf{x}_j' = (x_j',y_j')$ are the measured photo coordinates of the control points;
$\mathbf{X}_j = (X_j',Y_j',Z_j)$ are the corresponding known object-space coordinates;
$[A_n(\mathbf{x}_j',\mathbf{X}_j)]$ is the L.H.S. matrix whose elements are a function of the observed photo and object-space coordinates;
$\mathbf{b}_n(\mathbf{x}_j')$ is the R.H.S. column vector whose elements are a function of the observed photo-coordinates only; and
$\mathbf{L}^0 = (L_1{}^0,L_2{}^0, \ldots, L_{11}{}^0)$ is an initial approximation to the solution vector of the 11 DLT coefficients.

When the image coordinates of any unknown non-control point imaged on m photographs (i.e., $k=1,\ldots,m$), are substituted into Equations 10 in turn, the resulting set of $2m$ equations can be written similarly as

$$[C_m(\mathbf{x}_k',\mathbf{L}^0)]\ \mathbf{X}^0 = \mathbf{d}_m(\mathbf{x}_k',\mathbf{L}^0) \tag{12}$$

where $\mathbf{X}^0 = (X,Y,Z)$ is an initial approximation to the object space coordinates of a typical non-control point;
$[C_m(\mathbf{x}_k',\mathbf{L}^0)]$ is the L.H.S. matrix whose elements are a function of the observed photo coordinates of a non-control point and the associated DLT coefficients of the corresponding photograph; and
$\mathbf{d}_m(\mathbf{x}_k',\mathbf{L}^0)$ is the R.H.S. column vector whose elements are a function of the above stated parameters.

The trial solution $\mathbf{X}^i$ ($i=0,1,\ldots$) upon substitution into Equation 11, yields an updated set of DLT coefficients $\mathbf{L}^{i+1}$ ($i=0,1,\ldots$), which in turn produces a revised approximation to the object space coordinates $\mathbf{X}^{i+1}$ utilizing Equation 12. The iterative procedure is repeated until a converged solution is obtained.

Algorithmically, for $j = 1,\ldots,n$ control and $j = n+1,\ldots,N$ non-control points imaged on each photograph, the scheme can be represented by

$$[A_N(\mathbf{x}_j',\mathbf{X}_j^i)]\ \mathbf{L}^i = \mathbf{b}_N(\mathbf{x}_j') \tag{13}$$

and similarly, for every jth non-control point ($j = n+1,\ldots,N$) imaged in $k = 1,\ldots,m$ photographs by

$$[C_m(\mathbf{x}_k',\mathbf{L}_i]\ \mathbf{X}^{i+1} = \mathbf{d}_m(\mathbf{x}_k',\mathbf{L}^i) \tag{14}$$

Systematic non-linear corrections to image coordinates of the form

$$\mathbf{x}_j'^{i+1} = \mathbf{x}_j'^{i} + \Delta\mathbf{x}_j'^{i}$$

are neglected. Furthermore, the image coordinate vector $\mathbf{x}_j'$ ($j = 1,\ldots,N$) along with the corresponding object-space control point coordinates $\mathbf{X}_j^i$ ($j = 1,\ldots,n$) are maintained constant throughout the iterative procedure. However, the vector of calibration parameters $\mathbf{L}^i$ and the unknown object-space coordinates $\mathbf{X}_j^i$ ($j = n+1,\ldots,N$) are updated by successive approximations. Then in an ideal case, provided a suitable convergence criterion can be identified, the ILT scheme will converge in such a way that as i increases

$$\mathbf{X}_j^{i+1} \rightarrow \mathbf{X}_j^i;\ (j = n + 1, \ldots, N).$$

Wong (1975) demonstrated empirically that the diagonal elements of Equation 8 provide reliable estimates to the actual RMS errors of the elements of the solution vector to Equation 7, provided the iterative corrections are less than the computed RMS errors. Accordingly, let $(\sigma_{Xk}, \sigma_{Yk}, \sigma_{Zk})$ be the X, Y, Z components of the computed RMS error vector for the estimated object-space coordinates of point k ($k = 1,\ldots,N$), and define it's Euclidean length as

$$\sigma_{Pk} = (\sigma_{Xk}{}^2 + \sigma_{Yk}{}^2 + \sigma_{Zk}{}^2)^{1/2}$$

whence the average length of the RMS error vector is given by

$$\bar{\sigma}_P = \frac{1}{N}\sum_{k=1}^{N} \sigma_{Pk}$$

Then convergence can be monitored by ensuring satisfaction, for n_i successive iterations, of the criterion

$$\left| \bar{\sigma}_P{}^{i+1} - \bar{\sigma}_P{}^{i} \right| < \text{TOL} \tag{15}$$

In Equation 15, TOL is a specified tolerance value, and $\bar{\sigma}_p{}^i$ is $\bar{\sigma}_p$ at the *i*th iteration. Appropriate values for both TOL and n_i for the class of problem under investigation must now be determined empirically.

EXPERIMENTAL STUDIES OF ANALYTICAL RECONSTRUCTION

GENERAL

To investigate the performance of the ILT procedure, the following close-range photogrammetric studies have been undertaken:

- Reconstruction of check-point control - enabling a direct comparison of accurately coordinated and photogrammetrically reconstructed values for the same points.
- Half cylinder - a simple surface whose precise mathematical form is well defined.
- Breast surface of a mannequin - a complex shape for which no comparable solution is available.

The photographic images were obtained using a Hasselblad 500C/M non-metric camera in conjunction with the structured light technique (Renner, 1977; Frobin and Hierholzer, 1981; Lewis and Sopwith, 1986). In this method a well defined pattern is projected at the object-space control and surface to be reconstructed. A single photograph of the resulting distorted pattern then contains all the information for determination of that part of the surface visible to it. For the present application the structured light was a regular square grid, and Figure 1 shows a representative image so obtained (mannequin breast photo 2 and surrounding control-point configuration). Thus, the spatial points reconstructed comprise the object coordinates of the grid intersections and control points. Each photograph was digitized once manually; further details of the data aquisition system are described by Naftel (1989).

For each study two independent photogrammetric reconstructions have been obtained, thus enabling a number of separate statistical error measures to be used to study the accuracy of the results obtained. In the ensuing sections, therefore, the relevant error measures are first discussed prior to detailed consideration of the above-mentioned case studies.

DEFINITION OF CERTAIN USEFUL ERROR MEASURES

Let σ_{xk}, σ_{Yk}, σ_{Zk} be the *X*, *Y*, *Z* components of the RMS error (Wong, 1975) for point k ($k = 1, \ldots, N$). Then σ_{Pk}, the Euclidean length of the RMS error vector can be expressed as

$$\sigma_{Pk} = (\sigma_{Xk}{}^2 + \sigma_{Yk}{}^2 + \sigma_{Zk}{}^2)^{1/2} \tag{16}$$

whence the average Euclidean length of the RMS error vector is

$$\bar{\sigma}_P = \frac{1}{N} \sum_{k=1}^{N} \sigma_{Pk} \tag{17}$$

The magnitude of $\bar{\sigma}_P$ gives a statistical indication of the overall consistency of the data for any N reconstructed points, as determined by the least-squares adjustment process. However, we can expect $\bar{\sigma}_P$ to underestimate the reconstruction errors in an ILT solution for the object space coordinates. This is partly due to random and systematic sources of error in observed comparator (digitized) coordinates, and partly to the approximation implicit in the DLT equations (Fraser, 1982).

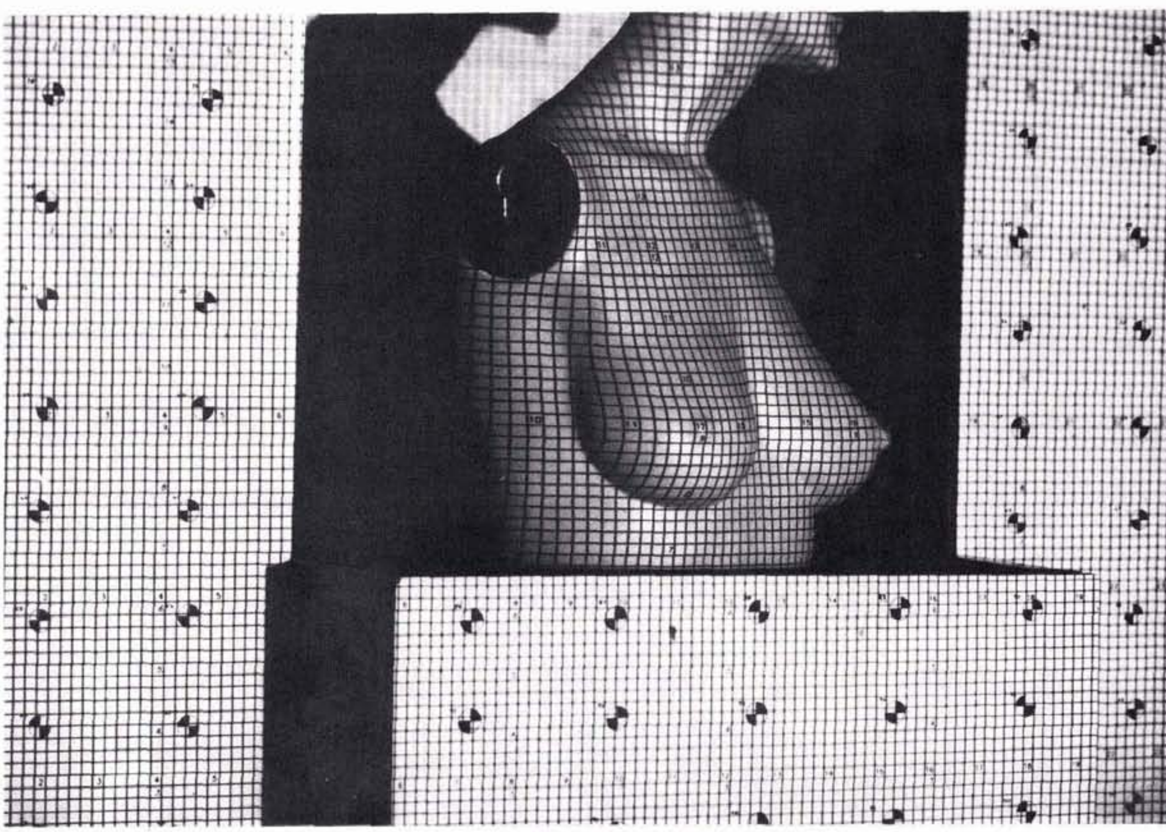

FIG. 1. Structured light image of mannequin breast.

Clearly, the residual or true error (r_{pk}) in any photogrammetrically reconstructed point (with computed coordinates X_{Ck}, Y_{Ck}, Z_{Ck}) can only be assessed if the true coordinates (X_{Tk}, Y_{Tk}, Z_{Tk}) are known; in this case, the average Euclidean length of the residual error vector $\bar{\mathbf{r}}_P$ of N_c such points can be similarly defined as

$$\bar{\mathbf{r}}_P = \frac{1}{N_c}\sum_{k=1}^{N_c}\{(X_{Tk} - X_{Ck})^2 + (Y_{Tk} - Y_{Ck})^2 + (Z_{Tk} - Z_{Ck})^2\}^{1/2} \quad (18)$$

The reconstruction of identical unknown object-space points from independent photographs facilitates the definition of a third error measure, known as the RMS deviation (to differentiate it from the RMS error). It can be shown (Taylor, 1982) that the RMS deviation for two observations x_1 and x_2 of a single quantity x, is given by $|x_1 - x_2|/\sqrt{2}$. Therefore, it follows that the X, Y, Z components (s_{Xk}, s_{Yk}, s_{Zk}) of the RMS deviation for two independent reconstructions of an unknown object-space point k are given by

$$\{s_{Xk}, s_{Yk}, s_{Zk}\} = \frac{1}{\sqrt{2}}\left\{\left|X_k' - X_k''\right|, \left|Y_k' - Y_k''\right|, \left|Z_k' - Z_k''\right|\right\} \quad (19)$$

where the prime and double prime are used to distinguish spatial coordinates determined from separate photographs. The average Euclidean length of the RMS deviation vector can now be written (*cf.* Equations 17 and 18) as

$$\bar{\mathbf{s}}_P = \frac{1}{N_p\sqrt{2}}\sum_{k=1}^{N_p}\{(X_k' - X_k'')^2 + (Y_k' - Y_k'')^2 + (Z_k' - Z_k'')^2\}^{1/2} \quad (20)$$

where N_p is the number of points common to separate reconstructions.

Reconstruction of Check-Point Control

The control points consisted of clearly visible target marks mounted on a rigid frame. In total, three independent coordinate evaluations were obtained for each of 58 controls using conventional theodolite survey techniques (Naftel, 1989). The average standard error for all the control point coordinates so obtained was 0.073mm, while the worst value for any point was 0.220mm. Therefore, under the assumption that the conventionally surveyed coordinates represent the "true" values, the accuracy of photogrammetrically reconstructed values for the same points can be assessed.

For the present study a total of 45 control points were employed, roughly mid-way between the upper (60) and lower (25) bounds suggested by Fraser (1982) and Karara and Abdel-Aziz (1974), respectively, from which smaller samples of 5, 10, and 15 points were drawn. These samples, evenly distributed thoughout the control space, were used as check point control. The results of the two independent reconstructions are summarized in Table 1.

For these numbers of unknown object points, the RMS errors converged to three decimal places with TOL = 5×10^{-4}, n_i = 5 in the total number of iterations shown. Figure 2 illustrates the effectiveness of the ILT procedure in reducing the errors in the initial DLT solution. It can be noted that convergence is rapid for all values of N_c. However, as the ratio of the number of control to "unknown" points falls, $\bar{\sigma}_P$ increases significantly with an associated decrease in the rate of convergence. Certainly there is no evidence in Table 1 to suggest that the optimum degree of redundancy (for accuracy) in control has been reached in this investigation.

Further inspection of Table 1 reveals that $\bar{\sigma}_P$ consistently underestimates $\bar{\mathbf{r}}_P$ (i.e., the "true" error), as anticipated previously, although the trends of the two error estimates are always the same. Analytical reconstruction of identical check point controls from the second photograph yields larger residual errors than the first, although averaging the reconstructions from both images enhances the accuracy of the ILT solution. Finally, we note that $\bar{\mathbf{s}}_p$ provides a good indication of $\bar{\mathbf{r}}_p$, which for the well defined target marks used here was on the order of 1 mm, a figure consistent with previously published results (Abdel-Aziz and Karara, 1974).

It can be appreciated from Equations 2 and 3 that the ADPs are readily incorporated into Equations 5 and 10 as additional "calibration" parameters together with the DLT coefficients. In an initial set of reconstruction studies to determine which of the ADPs were statistically significant, only the K_1 term (first component of symmetrical lens distortion) had any effect on the solution. The inclusion of the K_1 parameter can be applied to the final iteration of the ILT solution using an option in the standard program developed by Marzan and Karara (1975). A single iteration with the so-called 12th parameter proved sufficient, and the computed errors obtained including the K_1 term in the ILT procedure are shown in Table 2.

From a comparison of Tables 1 and 2, it is found that in the majority of cases there is a marked deterioration in the accuracy of the solution. Notable exceptions are an improvement in the residual errors for N_c=5 (photo 1) and N_c=15 (photo 2). Overall, however, on the basis of these results, there can be little justification for inclusion of the K_1 parameter in the ILT solution; using a healthy redundancy in control and assuming only linear distortion of image coordinates (which is automatically included in the solution for the DLT parameters) is the optimum procedure.

Reconstruction of Selected Test Surfaces

It can be seen from Table 3 that the much higher number of unknown spatial points encountered in these studies resulted in a correspondingly slower rate of convergence. Nevertheless, convergence of $\bar{\sigma}_p$ to a value of TOL = 5×10^{-4} for n_i = 10 successive iterations ensured that the corrections to the object space coordinates were less than the corresponding computed rms errors, as suggested by Wong (1975), in each case. Figure 3 illustrates the convergence paths obtained for both studies, which again demonstrate the effectiveness of the ILT algorithm in reducing the errors in the initial DLT solution assuming equal weights for all observations. At this stage, it is perhaps pertinent to re-emphasize the significance of the weight matrix in obtaining an optimum overall solution based on both the values and relative

Table 1. Comparison of Error Measures Using the ILT Solution for Reconstruction of Check Point Control

No. check controls	No. control points	No. iterns. n_i	$\bar{\sigma}_P$ (mm) photo 1	$\bar{\mathbf{r}}_P$ (mm) photo 1	$\bar{\mathbf{r}}_P$ (mm) photo 2	$\bar{\mathbf{r}}_P$ (mm) photos 1 & 2	$\bar{\mathbf{s}}_P$ (mm) photos 1 & 2
5	40	8	0.374	0.954	–	–	–
10	35	9	0.672	0.985	–	–	–
15	30	16	0.732	1.095	1.320	0.972	1.118

TABLE 2. DEMONSTRATION OF THE EFFECT OF INCLUDING THE K_i PARAMETER ON THE RESULTS PRESENTED IN TABLE 1.

No. check controls	No. control points	No. iterns. n_i	$\bar{\sigma}_P$ (mm) photo 1	$\bar{r}_P$ (mm) photo 1	$\bar{r}_P$ (mm) photo 2	$\bar{r}_P$ (mm) photos 1 & 2	$\bar{s}_P$ (mm) photos 1 & 2
5	40	9	0.551	0.868	—	—	—
10	35	10	0.764	1.123	—	—	—
15	30	17	0.895	1.317	1.310	1.018	1.334

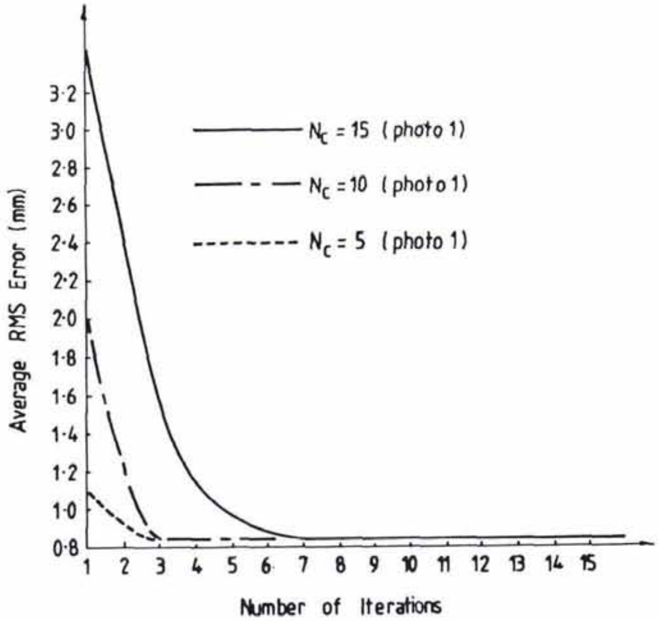

FIG. 2. Convergence of ILT solution for analytical reconstruction of check point control.

accuracies of control and non-control points: attempts to obtain ILT solutions more cheaply by retaining a unit weight matrix for all iterations have consistently lead to divergence.

In the absence of check-point controls, $\bar{s}_P$ is believed to be the most reliable available estimate of accuracy. Again, it can be noted that $\bar{\sigma}_P$ is always less than $\bar{s}_P$ while the trends of the two error estimates are the same. Comparison of the error estimates in Tables 1 and 3 suggests that the errors obtained in these studies were appreciably higher than those resulting from the check-point control studies. The main reason for this is thought to be that the grid line intersections produce less clearly identifiable points for manual digitization than control points, and consequently lead to larger random digitization errors. This effect is believed to increase with the shape complexity of the object surface, due to greater distortion of the structured light pattern. These matters are further discussed in the conclusions.

TABLE 3. RECONSTRUCTION OF TEST SURFACE MODELS (FIGURES IN BRACKETS ARE NUMBER OF GRID INTERSECTION POINTS VISIBLE IN BOTH PHOTOGRAPHS)

Test Object	Photo	No. Control points	No. surface points	No. iterns	$\bar{\sigma}_P$ (mm)	$\bar{s}_P$ (mm)
Cylinder	1	45	325	69	0.520	1.851
	2	45	326	140	0.521	(240)
Mannequin	1	45	117	47	0.744	2.092
	2	44	117	50	0.621	(39)

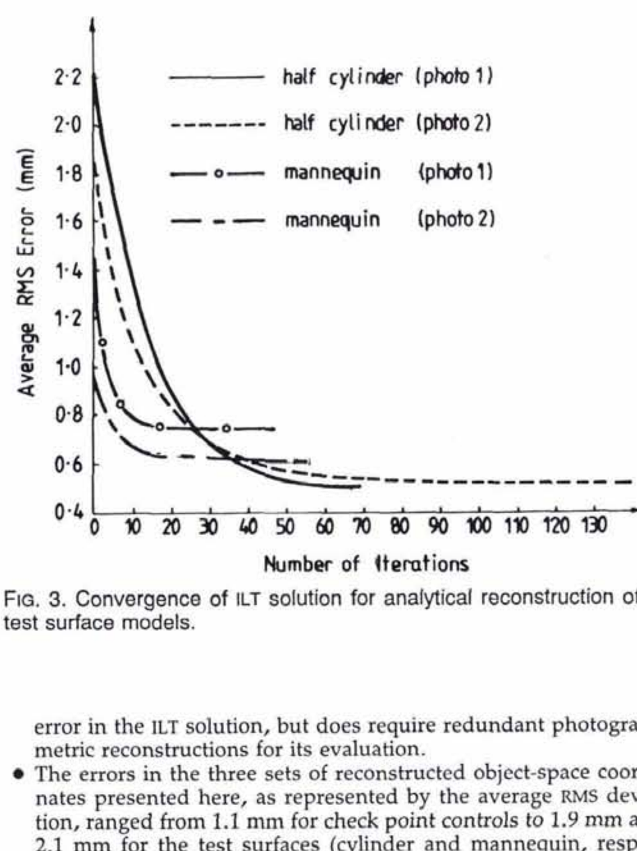

FIG. 3. Convergence of ILT solution for analytical reconstruction of test surface models.

CONCLUSIONS

- The iterative linear transformation (ILT) procedure, as described in the main body of this paper, has yielded converged solutions to all studies undertaken. Furthermore, the solutions so obtained have all exhibited considerably reduced rms errors in comparison to the original direct linear transformation (DLT) results.
- The computed RMS error of the converged solution derived from the variance-covariance matrix consistently overestimates the degree of accuracy achieved by the ILT solution. However, it can be used both to monitor convergence and as a guide to the underlying trend of the "true" (residual) error.
- The RMS deviation provides a more reliable indication of the "true" error in the ILT solution, but does require redundant photogrammetric reconstructions for its evaluation.
- The errors in the three sets of reconstructed object-space coordinates presented here, as represented by the average RMS deviation, ranged from 1.1 mm for check point controls to 1.9 mm and 2.1 mm for the test surfaces (cylinder and mannequin, respectively). These equate to spatial resolutions of 0.047 percent, 0.090 percent, and 0.096 percent, respectively. The larger errors incurred in the latter reconstructions are believed to be primarily due to manual digitization of the structured light procedure used in this study, and are not a function of the ILT procedure.
- The Iterative Linear Transformation (ILT) algorithm is an extremely useful procedure for solution of the collinearity equations in close-range photogrammetry where the provision of highly redundant object-space control presents no problems. Under these conditions accuracy achieved using this method is not significantly inferior to that obtained using techniques requiring both an initial approximation to the unknown parameters and much greater computer resources.

REFERENCES

Abdel-Aziz, Y. I., and H. M. Karara, 1971. Direct linear transformation from comparator coordinates into object space coordinates. *Proc. ASP/UI Symp. on Close-range photogrammetry*, Urbana, Illinois, pp. 1–18.

Alem, N. M., J. W. Melvin, and G. L. Holstein, 1978. Biomechanics applications of direct linear transformation in close-range photogrammetry. *Proc. 6th New Engl. Bioeng. Conf.*, Kingston, Rhode Island (Ed. Jason, D.). Pergamon press, pp. 202–206.

Bopp, H., and H. Krauss, 1977. A simple and rapidly converging orientation and calibration method for non-topographic applications. *Proc. ASP, Fall Tech. Meet.*, pp. 425–432.

Fraser, C. S., 1982. On the use of non-metric cameras in analytical close-range photogrammetry. *Canad. Surv.*, 36(3), 259–279.

Frobin, W., and E. Hierholzer, 1981. Rasterstereography: A photogrammetric method for measurement of body surfaces. *Photogrammetric Engineering & Remote Sensing*, 47(12), 1717–24.

Granshaw, S. I., 1980. Bundle adjustment methods in engineering photogrammetry. *Photogramm. Rec.*, 10(56), 181–207.

Hatze, H., 1988. High-precision three-dimensional photogrammetric calibration and object space reconstruction using a modified DLT-approach. *J. Biomech.*, 21(7), 533–538.

Karara, H. M., and Y. I. Abdel-Aziz, 1974. Accuracy aspects of non-metric imageries. *Photogrammetric Engineering & Remote Sensing*, 40(9), 1107–1117.

Lewis, J. R. T., and T. Sopwith, 1986. Three-dimensional surface measurement by microcomputer. *Image and Vision Comput.*, 4(3), 159–166.

Marzan, G. T., and H. M. Karara, 1975. A computer program for direct linear transformation solution of the collinearity condition, and some applications of it. *Proc. ASP Symp. on Close-range Photogrammetric Systems*, Illinois, pp. 420–476.

Miller, N. R., R. Shapiro, and T. M. McLaughlin, 1980. A technique for obtaining spatial kinematic parameters of segments of biomechanical systems from cinematographic data. *J. Biomech.*, 13, 535–547.

Naftel, A. J., 1989. *Three-Dimensional Techniques for the Geometric Study of Expanded Skin Surfaces*. PhD Thesis, University of Bradford, U.K.

Renner, W. D., 1977. A photogrammetric technique for use in radiation therapy. *Photogrammetric Engineering & Remote Sensing*, 43(5), 581–591.

Shapiro, R., 1978. Direct linear transformation method for three-dimensional cinematography. *Res. Quart.*, 49, 197–205.

Taylor, J. R., 1982. *An Introduction to Error Analysis. The Study of Uncertainties in Physical Measurements*. University Science Books.

Van Gheluwe, B., 1978. Computerised three-dimensional cinematography for any arbitrary camera set-up. *Biomechanics VI-A*. (E. Asmussen and K. Jorgensen, eds.) University Park Press, pp. 343–348.

Wong, K. W., 1975. Propogation of variance and covariance. *Photogrammetric Engineering & Remote Sensing*, 41(1), 75–89.

Wood, G.A., and R.N. Marshall, 1986. Accuracy of DLT extrapolation in three-dimensional film analysis. *J. Biomech.*, 19(9), 781–785.

(Received 17 March 1990; revised and accepted 19 October 1990)